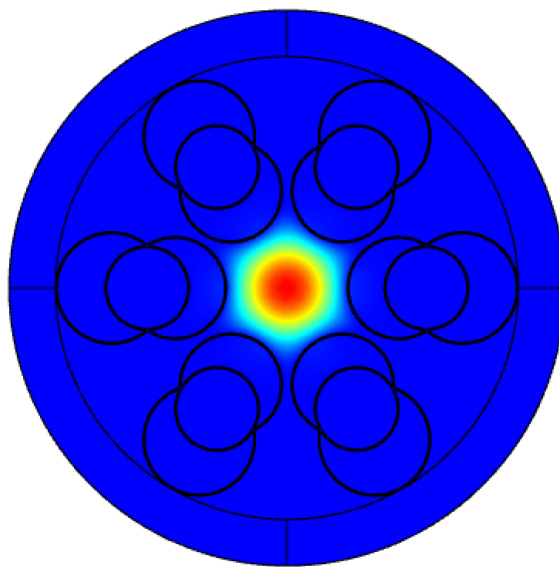


Low Loss Hollow-Core Connecting-Circle Negative-Curvature Fibres

Volume 13, Number 1, February 2021

Boyi Yang
Xuesheng Liu
Wenzeng Jia
Shu Liu
Kai Mei
Tingwu Ge
Dengcai Yang
Youqiang Liu
Tian Lan
Zhiyong Wang



DOI: 10.1109/JPHOT.2021.3052947

Low Loss Hollow-Core Connecting-Circle Negative-Curvature Fibres

Boyi Yang, Xuesheng Liu , Wenzeng Jia, Shu Liu, Kai Mei, Tingwu Ge , Dengcai Yang, Youqiang Liu, Tian Lan, and Zhiyong Wang

¹Beijing Engineering Research Center of Laser Technology, Beijing University of Technology, Beijing 100124, China

²Key Laboratory of Trans-scale Laser Manufacturing Technology, (Beijing University of Technology), Ministry of Education, Beijing 100124, China

³Institute of Advanced Technology on Semiconductor Optics & Electronics, Institute of Laser Engineering, Beijing University of Technology, Beijing 100124, China

DOI:10.1109/JPHOT.2021.3052947

This work is licensed under a Creative Commons Attribution 4.0 License. For more information, see <https://creativecommons.org/licenses/by/4.0/>

Manuscript received December 15, 2020; revised January 15, 2021; accepted January 16, 2021. Date of publication January 19, 2021; date of current version February 10, 2021. This work was supported in part by the Science and Technology on Solid-State Laser Laboratory Open Fund and in part by the National Key Research and Development Program of China under Grant 2017YFB0305800. Corresponding author: Xuesheng Liu (e-mail: liuxuesheng@bjut.edu.cn).

Abstract: Hollow-core negative-curvature fibres have been the focus of current research, but how to reduce the loss of hollow-core negative-curvature fibres is a serious problem. This paper proposes a new structure of hollow-core negative-curvature fibres, that is numerically simulated using the finite-element method, and compared with the simulation results of hollow-core conjoined-tube negative curvature fibres (CTNCFs) and hollow-core nested anti-resonant nodeless fibres (NANFs). The results show that, the LP_{01} mode loss can reach 0.003694 dB/km with a transmission wavelength of 1.06 μm , the LP_{11} mode loss can be as low as 0.28423 dB/km, and the bending loss is 0.4405 dB/km with a bending radius of 5 cm and a transmission wavelength of 1.06 μm . The loss is reduced by an order of magnitude compared to CTNCFs and NANFs.

Index Terms: Hollow-core negative-curvature fibres, anti-resonant, ultralow loss.

1. Introduction

The first kind of hollow-core fibres was hollow-core photonic band gap fibres (HC-PBGFs), which are divided into two-dimensional photonic bandgap fibres [1] and omniguide photonic bandgap fibres [2]. The laser will be transferred without nonlinear effects and dispersion in the quasi-vacuum optical environment [3], and HC-PBGFs have a wide range of applications in nonlinear optics [4], [5], ultrafast optics [6], and high power lasers [7]. However, due to the defect of the HC-PBGF itself, the basic loss called surface scattering cannot be eliminated [8], thus, it is not worth continuing to research, and any kind of high-performance hollow-core fibres must effectively reduce the spatial overlap between the mode field and the glass surface [9]. Based on these two considerations, academia has turned to hollow-core negative-curvature fibres as the research object [10].

Hollow-core negative-curvature fibres are based on the HC-PBGF, in which the cladding structure in the HC-PBGF is simplified to one cladding structure [11], the fibres can still transfer the laser, and the transmission mechanism is the anti-resonant reflection optical waveguide (ARROW) [12],

[13]. Unlike the complex cladding structure of HC-PBGFs, the hollow-core negative-curvature fibres have a simple cladding structure, and the transmission loss is low, thus, they have huge application potential in power transmission [14], data communication [15], and fibres lasers [16].

In 2011, Pryamikov A D *et al.* first proposed a glass hollow-core fibre. The curvature of the core wall is negative, and the transmission loss is 11 dB/m with a transmission wavelength of 10.6 μm [11]. In 2012, Yu F of the University of Bath in the United Kingdom proposed a hollow-core negative-curvature fibres similar to an ice cream structure, and the minimum loss of the fibres at a transmission wavelength of 3050 nm was 34 dB/km [17], which reduced the loss to less than 100 dB/km.

In 2018, Wang Y Y of the Institute of Laser Engineering of Beijing University of Technology devised a new structure of hollow-core negative-curvature fibres, when the transmission wavelength is 1512 nm, its lowest loss reaches 2.0 dB/km [3], which reduces the loss to less than 10 dB/km. In 2020, Debord B of the University of Southampton reduced the loss of hollow-core negative-curvature fibres to 0.28 dB/km by adding a circular nested tube, which is currently the lowest loss among hollow-core negative-curvature fibres [18], which reduced the loss to less than 1 dB/km.

Although the loss of hollow-core negative-curvature fibres is gradually decreasing, the current high transmission loss is still the main factor limiting the commercialization of hollow-core negative-curvature fibres. At present, the methods to reduce the transmission loss of hollow-core negative-curvature fibres mainly include adding nested tubes into the cladding tube [19] and CTNCFs. In this paper, we combine the virtues of NANFs and CTNCFs, and add a circular nested tube to the conjoined tube, to study its performance in reducing the loss and bending loss. We name it a hollow-core connecting-circle negative-curvature fibre (HC-CCNCF or CCNCF). From the simulation results, it has record-breaking low LP_{01} and LP_{11} mode loss, not only is the structure relatively simple, but also, it is possible to realize drawing. Finally, we calculate the higher order mode extinction ratio (HOMER), which has a high value, and can provide effective single-mode operation. Therefore, we believe that the CCNCF will break the record for ultralow loss hollow-core negative-curvature fibres with the possibility of drawing success.

2. Fibres Structure

Fig. 1, presents the structure of the fibres. The cladding of the fibres is composed of 6 noncontact connecting circles, which surround the air core with $D = 30 \mu\text{m}$. One of the cladding tubes is composed of two connecting circles with a small nested circle, and the structure of the cladding tube from (1) to (7) consists of an anti-resonant wall, a large moon-shaped air hole, an anti-resonant wall, a circular air hole, an anti-resonant wall, a small moon-shaped air hole, and an anti-resonant wall.

Because the connecting structure of circle 1 and circle 2 has a node, circle 3 can nest at the node, which is different from the ordinary nested structure, there is innovative. This is the advantage of CCNCF over complex nested structures [20].

Next, the fibre structural parameter settings are discussed. Kolyadin AN *et al.* proved that the produced extra resonance can be reduced when capillary tubes are separated from each other [21], so the distance between the circles 2 should be enhanced. The larger the diameter of the cladding tube relative to the core diameter is, the easier mode coupling occurs [22]. Based on these two considerations, and using COMSOL to simulate circle 1, circle 2, and circle 3 under different diameters and distances between the centres of circle 1 and circle 2, finally, the lowest loss is obtained with diameters d_1 , d_2 , and d_3 and distance l between the centre of circle 1 and circle 2 of 23 μm , 21.5 μm , 18.2 μm , 13.29 μm . When the anti-resonant wall thickness and the wavelength of the transmitted laser reach the anti-resonant condition, the loss of the fibres will be lower, and COMSOL is used to calculate the loss of the fibres under different anti-resonant wall thicknesses, The lowest loss is obtained with a transmission wavelength of 1.06 μm and an anti-resonant wall thickness of 0.35 μm .

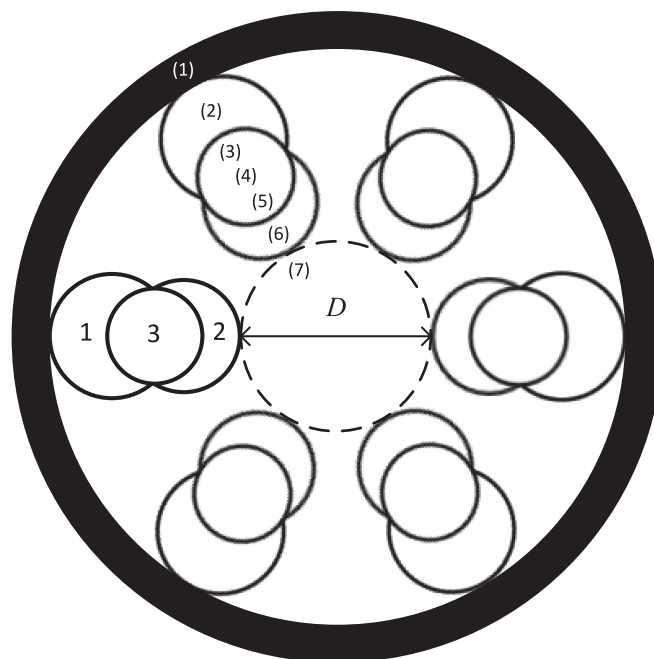


Fig. 1. CCNCF structure.

TABLE 1
Parameters of the Sellmeier Equation

$B_1=0.696\ 166\ 3$	$B_2=0.407\ 942\ 6$	$B_3=0.897\ 479\ 4$
$\lambda_1=0.068\ 404\ 3$	$\lambda_2=0.068\ 404\ 3$	$\lambda_3=0.068\ 404\ 3$

For the material part of the fibres, the white part is full of air with a refractive index n_{air} of 1, and the black part is silica, whose refractive index n_{silica} is determined by the Sellmeier equation: [23]

$$n_{silica}^2(\lambda) = 1 + \sum_{j=1}^m \frac{B_j \lambda^2}{\lambda^2 - \lambda_j^2} \quad (1)$$

λ_j is the j th resonant wavelength, B_j is the strength of the j th resonant wavelength, and λ is the transmission wavelength, generally, we use the first three items. The specific parameters are given in Table 1.

3. Simulation Results

3.1 Loss

The finite element method is used to calculate the loss of the fibres. Since the simulation result does not represent the real result, to reflect the superiority of the CCNCF, the NANF and CTNCF are simulated under the same simulation parameters, and the loss is calculated for comparison. Fig. 2. and Fig. 3, present the structures of the NANF and CTNCF.

The structural parameters of the NANF and CTNCF were obtained from references [3], [18], in NANF, $D_{NANF} = 37.2\ \mu\text{m}$, $d_{N1} = 23\ \mu\text{m}$, $d_{N2} = 10.5\ \mu\text{m}$, $t_N = 0.35\ \mu\text{m}$. In CTNCF, $D_{CTNCF} = 30.5\ \mu\text{m}$, the first layer of D-shaped air holes with the area of $S_1 = 270\ \mu\text{m}^2$, the second layer of D-shaped air holes with the effective area of $S_2 = 335\ \mu\text{m}^2$, $t_C = 0.35\ \mu\text{m}$. The only change is the

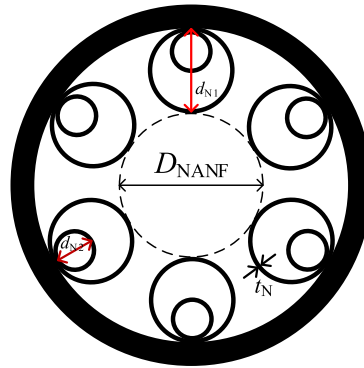


Fig. 2. NANF structure

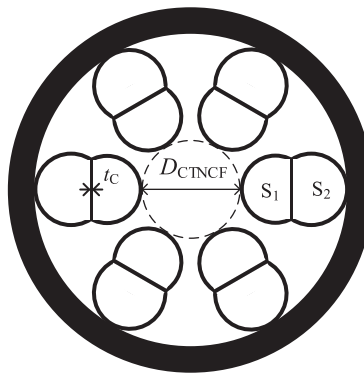


Fig. 3. CTNCF structure.

thickness of the anti-resonant wall, and the thicknesses of all the anti-resonant walls in these two fibres are all $0.35 \mu\text{m}$. In terms of material settings, in these two types of fibres, the black part is silica, and its refractive index n_{silica} is determined by the Sellmeier equation [17]. The white part is air, and its refractive index n_{air} is 1.

The CCNCF, NANF and CTNCF are simulated within the transmission band of $0.8\sim 1.6 \mu\text{m}$. Since the LP_{01} mode loss of these three kinds of fibres is very low, the loss of their LP_{11} mode is researched here. Fig. 4, presents the loss curves of the LP_{01} mode and the loss of the LP_{11} mode of the three types of fibres.

According to the simulation results, compared with the NANF and CTNCF, the CCNCF reduces the loss of the LP_{01} mode by an order of magnitude for the transmission wavelengths of $0.8\sim 1.6 \mu\text{m}$. Compared with the NANF, the CCNCF reduces the loss of the LP_{11} mode by an order of magnitude, and compared with the CTNCF, the CCNCF reduces the loss of the LP_{11} mode by several orders of magnitude. This shows that the performance of the CCNCF in reducing the loss of the LP_{01} mode and LP_{11} mode is better than that of the NANF and CTNCF. When the transmission wavelength is $1.06 \mu\text{m}$, the LP_{01} mode loss of the CCNCF can reach as low as 0.003694 dB/km . Table 2 shows the comparison of the lowest loss among the CCNCF, NANF and CTNCF.

3.2 Single-Mode Characteristics

The single-mode characteristics of the hollow-core negative-curvature fibres are represented by the HOMER, and the definition of the HOMER is the ratio of the lowest loss of the higher order mode to the loss of the LP_{01} mode under the same structure parameters. In this research, through

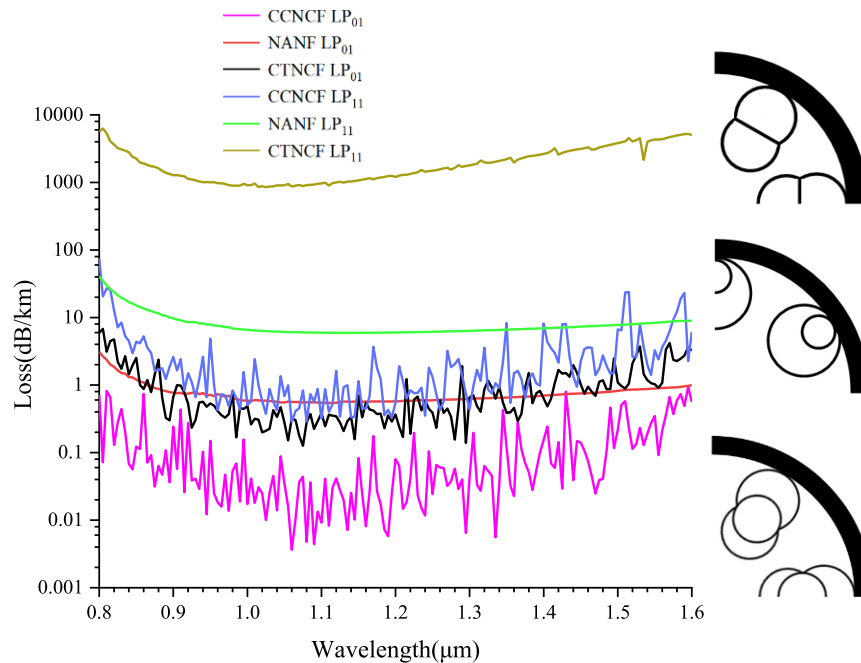


Fig. 4. LP_{01} and LP_{11} mode losses of the CCNCF, NANF and CTNCF in the 0.8~1.6 μm transmission band.

TABLE 2
Lowest Loss of the LP_{01} Mode and LP_{11} Mode of the Three Types of Fibres

Fibres type	Wavelength at the lowest loss (μm)	Lowest loss in LP_{01} mode (dB/km)	Wavelength at the lowest loss (μm)	Lowest loss in LP_{11} mode (dB/km)
CTNCF	1.06	0.31905	1.06	871.61
NANF	1.1	0.5483	1.15	5.9447
CCNCF	1.06	0.003694	1.06	0.28423

the simulation result, we can obtain that the higher-order modes with the lowest loss of the three structures of the fibres are all the LP_{11} modes. Fig. 5, presents the HOMER curves of the three fibres and the mode fields of the LP_{01} mode and the LP_{11} mode when the transmission wavelength is 1.06 μm for the three different fibre structures.

Through the curves, we can obtain that the CTNCF has the best single-mode performance, and the value of the HOMER is much higher than those for the CCNCF and NANF. The single-mode characteristics of the CCNCF are slightly better than those of the NANF, which is a deficiency of the CCNCF.

Because CCNCF is designed to obtain lower losses of LP_{01} and LP_{11} modes, we calculate HOMER between another lowest loss higher-order mode and the LP_{11} mode. As is shown in Fig. 6.

We can obtain that the HOMER between LP_{12} mode and LP_{11} mode are higher than 300. Therefore, we believe that CCNCF has a good inhibitory effect on the other higher-order modes.

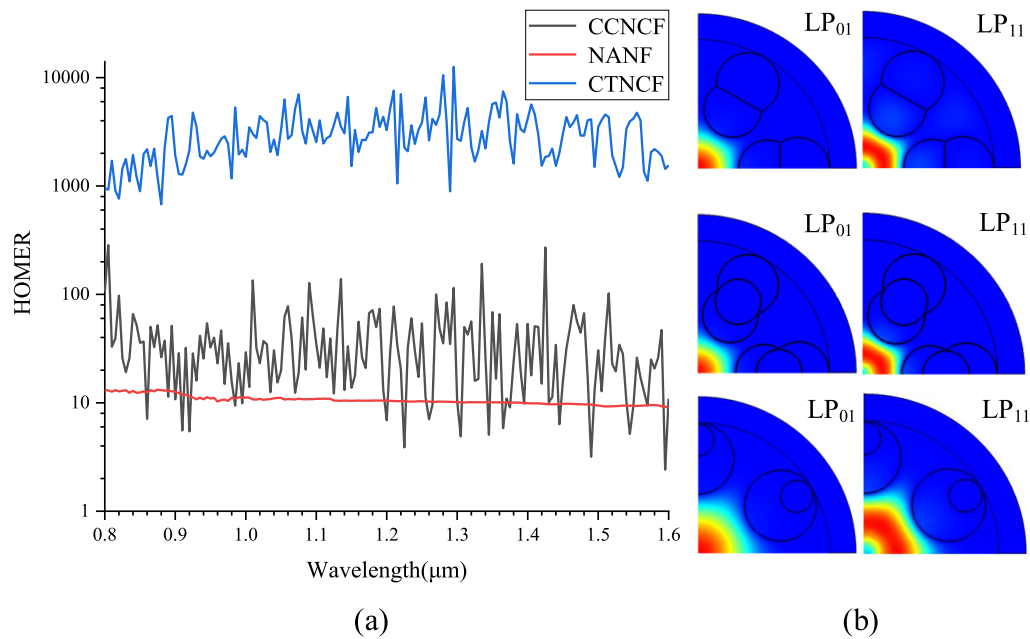


Fig. 5. (a) HOMER curves of the CTNCF, CCNCF and NANF. (b) LP₀₁ mode of the CTNCF, CCNCF and NANF, and LP₁₁ mode of the CTNCF, CCNCF and NANF.

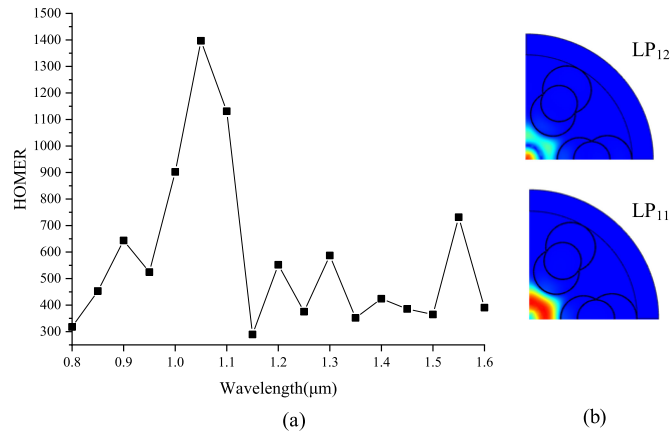


Fig. 6. (a) HOMER between LP₁₂ mode and LP₁₁ mode. (b) LP₁₂ and LP₁₁ modes of the CCNCF.

3.3 Bending Loss

The bending loss is also another important characteristic of fibres. Research has shown that reducing the core diameter can reduce the bending loss [10], [24], which is also the reason why the CCNCF core diameter is 30 μm. We use the conformal transformation method [25] to calculate the bending loss, using the formula:

$$n'(x, y) = n(x, y) \exp(x/R_{bend}) \quad (2)$$

where $n'(x, y)$ is the conformal index distribution, $n(x, y)$ is the index distribution before bending, R_{bend} is the bending radius, and x is the transverse distance from the centre of the fibre.

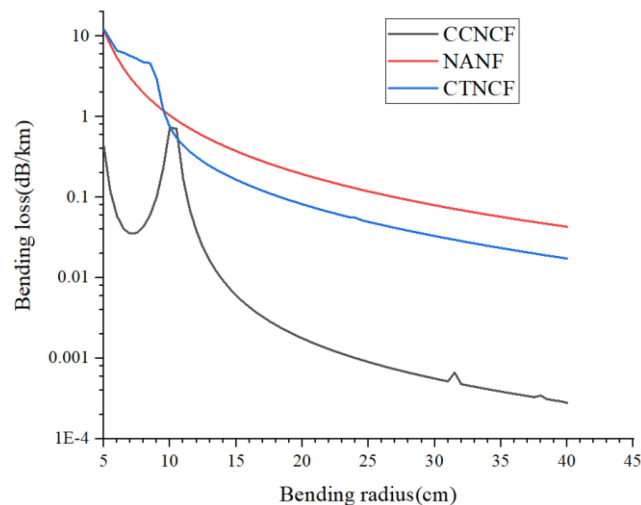


Fig. 7. Bending loss curves of the NANF, CCNCF and CTNCF.

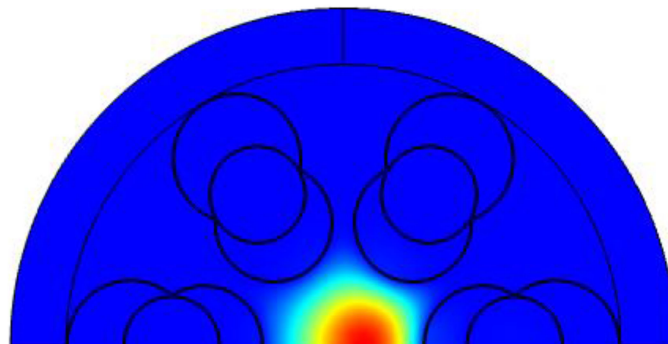


Fig. 8. Mode field of the bent CCNCF at a bending radius of 5 cm.

We assume that the fibre is bent in the x direction. We have calculated the bending losses of the NANF, CCNCF and CTNCF, the structural parameters of the NANF and CTNCF are both from references [3], [18], and the structural parameters of the CCNCF are from part 1, which give a lower loss at the transmission wavelength of $1.06 \mu\text{m}$. Fig. 7, presents the bending loss curves of the NANF, CCNCF and CTNCF with bending radii of $5\sim 40$ cm. We can obtain that with an increase in the bending radius, the bending loss of the CCNCF, CTNCF, and NANF is gradually reduced, because, as the bending radius increases, the offset of the bending mode field decreases. Through the numerical comparison of the bending losses of the CCNCF, CTNCF and NANF, we can obtain that the CCNCF is far better than the CTNCF and NANF in reducing the bending loss. Under the same simulation conditions, the CTNCF can reduce the bending loss by an order of magnitude.

Fig. 8, presents the mode field of the bent CCNCF at a bending radius of 5 cm, and we can obtain that the mode field of the curved CCNCF shifts in the bending direction.

4. Discussion

Due to the limitations of the current drawing manufacturing technology, the cladding tube can only be designed to be a circle, but the elliptical structure of the cladding tube has greater potential [26], lower loss, and more variable structures. If the drawing technology becomes mature, then designing the cladding tube into an elliptical structure will further reduce the loss of the fibres. We

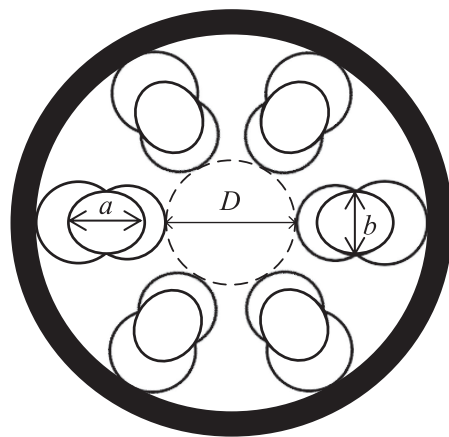
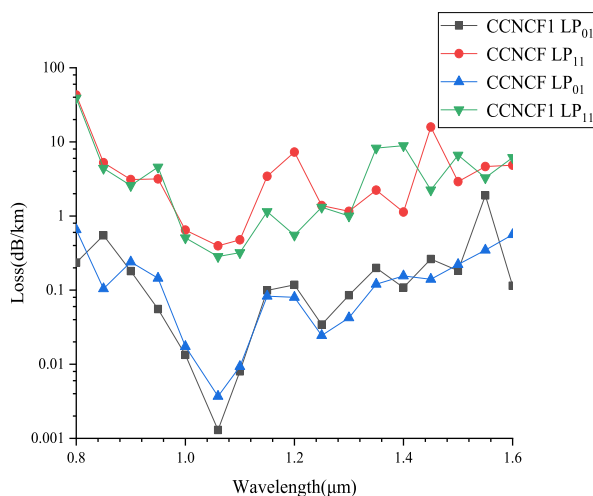


Fig. 9. CCNCF1 structure.

Fig. 10. LP₀₁ mode and LP₁₁ mode loss change for the CCNCF and CCNCF1 in the transmission band of 0.8~1.6 μm.

slightly change the structure, for example, if circle 3 is changed to an ellipse, where the minor axis length b is the same as the diameter of original circle 3, and the major axis length a is changed to 19.2 μm, then the modified fibres is named CCNCF1. Fig. 9, presents its structure.

Fig. 10, presents the loss of the LP₀₁ mode and LP₁₁ mode of CCNCF1 and the CCNCF at wavelengths of 0.8~1.6 μm.

We can obtain from the curve that although the loss curve of CCNCF1 is close to the loss curve of the CCNCF, the lowest LP₀₁ and LP₁₁ mode losses of CCNCF1 are both lower than those of the CCNCF, and the lowest LP₀₁ mode loss reaches 0.001 dB/km. It is proven that the elliptical structure has great potential in reducing the loss.

We have noticed that there is a 2-bar CTF in paper [3], which is similar to CCNCF. Fig. 11, presents the approximate structure. In the 2-bar CTF, $D_1 = 30.5$ μm, the first layer of semicircular air holes with the area of $s_1 = 278$ μm², the second layer of rectangle air holes with the effective area of $s_2 = 455$ μm², the third layer of semicircular air holes with the area of $s_3 = 278$ μm², $t_1 = 0.35$ μm.

Since the two proposed designs have the same number of antiresonant layer, the 2-bar CTF and CCNCF are simulated under the same condition, and the loss is calculated for comparison.

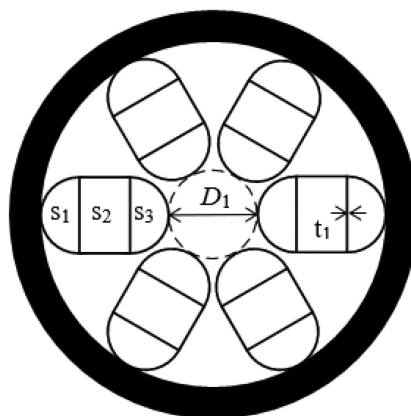


Fig. 11. 2-bar CTF structure.

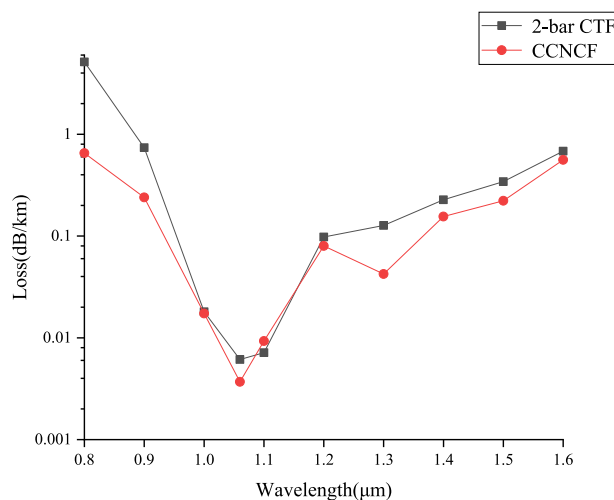
Fig. 12. The losses of the LP_{01} mode of the 2-bar CTF and the CCNCF at wavelengths of 0.8~1.6 μm .

Fig. 12, presents the losses of the LP_{01} mode of the 2-bar CTF and the CCNCF at wavelengths of 0.8~1.6 μm .

We can obtain from the curve that although the loss curve of the 2-bar CTF is close to the loss curve of the CCNCF, the lowest LP_{01} loss of CCNCF is lower than 2-bar CTF. It is proved that the negative curvature antiresonant bar has some advantages.

5. Conclusion

This article introduces a new kind of hollow-core negative-curvature fibres, and uses the finite element method to simulate and calculate the loss, compared with those of the NANF and CTNCF under the same conditions. Finally, the LP_{01} mode loss of the CCNCF is approximately an order of magnitude lower than those of the NANF and CTNCF. The loss of the CCNCF can be reduced to 0.003964 dB/km with a transmission wavelength of 1.06 μm , the LP_{11} mode loss can be as low as 0.28423 dB/km, and the bending loss is 0.4405 dB/km with a bending radius of 5 cm and a transmission wavelength of 1.06 μm . The single-mode characteristics of the CCNCF are slightly better than those of the NANF but worse than those of the CTNCF. And the HOMER between LP_{12}

mode and LP₁₁ mode are higher than 300. We provide a solution to reduce the loss of the hollow-core negative-curvature fibre. More work is needed to increase the loss of LP₁₁ modes without penalizing the LP₀₁ mode, and to keep the losses of LP₀₁ and LP₁₁ flat in the whole transmission window.

References

- [1] J. Knight, "Photonic crystal fibers," *Nature*, vol. 424, pp. 847–851, 2003.
- [2] G. J. Steven *et al.*, "Low-loss asymptotically single-mode propagation in large-core omniguided fibers," *Opt. Exp.*, vol. 9, pp. 748–779, 2001.
- [3] S. F. Gao *et al.*, "Hollow-core conjoined-tube negative-curvature fibre with ultralow loss," *Nat. Commun.*, vol. 9, no. 1, pp. 2–4, 2018.
- [4] P. S. Russell *et al.*, "Hollow-core photonic crystal fibers for gas-based nonlinear optics," *Nat. Photon.*, vol. 8, pp. 278–286, 2014.
- [5] F. Couny *et al.*, "Generation and photonic guidance of multi-octave optical-frequency combs," *Science*, vol. 318, pp. 1118–1121, 2007.
- [6] T. Balciunas *et al.*, "A strong-field driver in the single-cycle regime based on self-compression in a Kagome fiber," *Nat. Commun.*, 2015, Art. no. 6117.
- [7] Y. Y. Wang *et al.*, "Hollow-core photonic crystal fiber for high power laser beam delivery," *High Power Laser Sci. Eng.*, vol. 1, no. 1, pp. 17–28, 2013.
- [8] P. J. Roberts *et al.*, "Ultimate low loss of hollow-core photonic crystal fibers," *Opt. Exp.*, vol. 13, pp. 236–244, 2005.
- [9] W. Ding *et al.*, "Research progress on light guiding mechanism and experimental fabrication of high-performance anti-resonant hollow-core fiber," *J. Phys.*, vol. 67, no. 12, pp. 50–67, 2018.
- [10] F. Yu and J. C. Knight, "Negative curvature hollow core optical fiber," *IEEE J. Sel. Topics Quantum Electron.*, vol. 22, no. 2, pp. 146–155, Mar./Apr. 2016, Art. no. 4400610.
- [11] A. D. Pryamikov *et al.*, "Demonstration of a waveguide regime for a silica hollow-core microstructured optical fiber with a negative curvature of the core boundary in the spectral region $>3.5 \mu\text{m}$," *Opt. Exp.*, vol. 19, no. 2, pp. 1441–1448, 2011.
- [12] J. L. Archambault, R. J. Black, S. Lacroix, and J. Bures, "Loss calculations for antiresonant waveguides," *J. Light Technol.*, vol. 11, pp. 416–423, 1993.
- [13] N. M. Litchinitser, A. K. Abeeluck, C. Headley, and B. J. Eggleton, "Antiresonant reflecting photonic crystal optical waveguides," *Opt. Lett.*, vol. 27, pp. 1592–1594, 2002.
- [14] M. Michieletto *et al.*, "Hollow-core fibers for high power pulse delivery," *Opt. Exp.*, vol. 24, pp. 7103–7119, 2016.
- [15] J. R. Hayes *et al.*, "Antiresonant hollow core fibers with octave spanning bandwidth for short haul data communications," in *Proc. Opt. Fibers Commun. Conf. Exhib.*, 2016, pp. 1–3.
- [16] M. R. Xu, F. Yu, and J. Knight, "Mid-infrared 1 W hollow-core fibers gas laser source," *Opt. Lett.*, vol. 42, pp. 4055–4058, 2017.
- [17] F. Yu, W. J. Wadsworth, and J. Knight, "Low loss silica hollow core fibers for 3–4 μm spectral region," *Opt. Exp.*, vol. 20, no. 10, 2012, Art. no. 11153.
- [18] G. T. Jasion and T. D. Bradley, "Hollow core NANF with 0.28dB/km attenuation in the c and l bands," in *Proc. OFC Opt. Fibers Commun. Conf. Expo.: OSA*, 2020, Paper Th4B.4.
- [19] W. Belardi and J. Knight, "Hollow antiresonant fibers with reduced attenuation," *Opt. Lett.*, vol. 39, no. 7, pp. 1853–1856, 2014.
- [20] M. S. Habib, O. Bang, and M. Bache, "Low-loss hollow-core silica fibers with adjacent nested anti-resonant tubes," *Opt. Exp.*, vol. 23, pp. 17394–17406, 2015.
- [21] A. N. Kolyadin *et al.*, "Light transmission in negative curvature hollow core fibers in extremely high material loss region," *Opt. Exp.*, vol. 21, no. 8, pp. 9514–9519, 2013.
- [22] X. Chen, X. W. Hu, and J. Y. Li, "Influencing factors of negative-curvature hollow-core fibers to loss," *Prog. Laser Optoelectron.*, vol. 56, no. 5, pp. 2–3, 2019.
- [23] J. B. Zhang, Z. F. Wang, and J. B. Chen, *Simulations of Negative Curvature Hollow-Core Fibers*. Shang Hai, China, 2014.
- [24] E. Marcatili and R. Schmeltzer, "Hollow metallic and dielectric waveguides for long distance optical transmission and lasers," *Bell Syst. Tech. J.*, vol. 43, no. 4, pp. 1783–1809, 1964.
- [25] M. Heiblum and J. H. Harris, "Analysis of curved optical waveguides by conformal transformation," *IEEE J. Quantum Electron.*, vol. 11, no. 2, pp. 75–83, Feb. 1975.
- [26] M. S. Habib, O. Bang, and M. Bache, "Low-loss single-mode hollow-core fibers with anisotropic anti-resonant elements," *Opt. Exp.*, vol. 24, no. 8, pp. 8429–8436, 2016.